Hindawi Publishing Corporation
Journal of Nanoscience
Volume 2016, Article ID 1361436, 8 pages
http://dx.doi.org/10.1155/2016/1361436

Research Article

Plasmachemical Synthesis of Nanopowders in the System Ti(O,C,N) for Material Structure Modification

Michael Filkov[1] and Andrei Kolesnikov[2]

[1]*VIESH Research Institute, 21st Veshnyakovsky Pr., Moscow 109456, Russia*
[2]*Department of Chemical, Metallurgical and Materials Engineering, Tshwane University of Technology, Private Bag X680, Pretoria 0001, South Africa*

Correspondence should be addressed to Andrei Kolesnikov; kolesnikova@tut.ac.za

Received 30 June 2016; Revised 5 September 2016; Accepted 8 September 2016

Academic Editor: Mingwang Shao

Refractory nanoparticles are finding broad application in manufacturing of materials with enhanced physical properties. Production of carbide, nitride, and carbonitride nanopowders in high volumes is possible in the multijet plasmachemical reactor, where temperature and velocity distributions in reaction zone can be controlled by plasma jet collision angle and mixing chamber geometry. A chemical reactor with three Direct Current (DC) arc plasma jets intersecting at one point was applied for titanium carbonitride synthesis from titanium dioxide, propane-butane mixture, and nitrogen. The influence of process operational parameters on the product chemical and phase composition was investigated. Mixing conditions in the plasma jet collision zone, particles residence time, and temperatures were evaluated with the help of Computational Fluid Dynamics (CFD) simulations. The synthesized nanoparticles have predominantly cubic shape and dimensions in the range 10–200 nm. Phase compositions were represented by oxycarbonitride phases. The amount of free (not chemically bonded) carbon in the product varied in the range 3–12% mass, depending on synthesis conditions.

1. Introduction

Various techniques have been investigated for the synthesis of high-purity titanium carbonitride nanoparticles. The ultimate goal of the developed technologies was to produce the stoichiometric titanium carbonitride powders having high purity, narrow particle size distribution, ultrafine particle size (<100 nm), and low content of free carbon.

The requirements for titanium carbonitride nanopowders used for manufacturing of advanced materials, mainly cutting tools and die parts, are quite stringent in terms of high chemical purity and narrow particle size distribution [1, 2]. Carbides, nitrides, and carbonitride nanoparticles are founding expanding applications in materials engineering and metallurgy, where in some cases the purity requirements are less demanding, especially in terms of free carbon content and oxygen impurities.

Nanopowders of various chemical compositions (oxides, carbides, nitrides, and oxycarbonitrides) with sizes below 100 nm are attracting wide attention of material scientists and engineers as inoculating agents (modificators). Wang et al. [3] have applied $TiC_{0.5}N_{0.5}$ ceramic nanoparticles as nucleating centers for the refinement of eutectic grains in Al-Si alloys. Orishich et al. [4] have demonstrated positive impact of titanium nitride nanoparticles on mechanical properties of laser-welded joints. The nanopowders in the systems TiCN and TiC(N,O) were successfully applied as inoculating agents for casted iron [5], inoculating agents for aluminium alloys [6, 7], steel and alloys dispersed inoculators [8], components of special coating used in metal alloy casting [9], and components of complex electrochemical coatings [10].

When molten alloys undergo solidification, the inoculating nanoparticles play a role of crystallization centers, and that leads to structure refinement and increase of mechanical properties of precast shapes and near-surface layers of machinery parts. Due to the fact that the amount of atoms in the surface layer of nanoparticles is of same order of magnitude as the amount of atoms in the whole particle volume,

the new effects, determined by laws of quantum mechanics, might play a role in interaction of nanoparticles with crystallizing media [11]. This is the area of extensive research where understanding of influence of nanoparticles physical and chemical properties on the bulk materials structure creation and life-cycle evolution still requires more experimental facts. As a contribution in this direction, in the current work titanium carbonitride nanopowders were synthesized in a multijet plasma reactor for further application as inoculating agent for metals and alloys and additive in a composite material using relatively inexpensive raw materials [12].

Different techniques for titanium carbonitride nanopowder manufacturing have been developed.

They include

(1) chemical reduction of titanium oxide, titanium chloride, or titanium hydride by carbon, nitrogen, and ammonia in high-temperature flow [13–15],

(2) chemical vapor deposition process [16],

(3) carbothermic reduction in molten salt [17] and carbothermal reduction-nitridation [18],

(4) sol-gel titanium dioxide reduction in carbon tube furnace [19],

(5) reaction ball milling [20].

Amongst listed methods of titanium carbonitride nanopowder synthesis, chemical synthesis in plasma reactors attracts attention due to high production rate and fast reaction time [21]. In recent years plasma technology was extensively used for refractory nanoparticles synthesis.

Plasmachemical synthesis of titanium carbonitride nanopowder was carried out in the DC plasma reactor using TiO_2 and C_3H_8 as raw material [22]. Precursor titania powder (particle size below 20 microns) feed rate varied in the range 1.2–3.6 kg/h with energy consumption of 36–60 kW.

Grabis and Zalite [23] used titanium hydride (precursor size 20–40 microns) to produce TiCN nanopowder in radiofrequency (RF) plasma jet reactor. Feed rate of titanium hydride was 0.9–1.2 kg/h at plasma power input of 60–100 kW. Authors of the papers [24, 25] used RF plasma reactor to synthesize titanium carbonitride nanopowders from Ti metal precursor in nitrogen plasma. Precursor metallic powder feed rate varied in the range 1.1–2.0 kg/h with energy consumption of 60–100 kW [25].

Evaporation of micron-sized raw TiCN particles and following condensation were carried out in microwave plasma reactors by Ermakov [26] and Leparoux et al. [27]. Leparoux et al. [28] used microwave plasma with power input 16.5 kW to process titanium powder (precursor size 1.5 microns) at the flow rates 0.114–0.168 kg/h.

Titanium dioxide was used by McFeaters et al. [29] as raw material for TiC synthesis in RF argon-hydrogen plasma with addition of methane as carburizer.

The obtained powders had

(a) cubic shape and particle size distribution in the range 10–200 nm;

(b) fixed carbon content below 9% mass;

(c) specific surface area in the range 20–50 m^2/g;

(d) monophase titanium carbonitride as well as two phases of titanium carbonitride [23].

The highest achieved production rate was 1.2 kg/h using RF plasma torch and titanium hydride as raw material. Because of further problems with chlorine gas utilization, most interesting are the processes without usage of chlorides, that is, processes where solid raw materials are used.

In plasma flow, conversion of solid raw material into nanosized products occurs via heating, melting, and evaporation of solid raw particles, with concurrent homogeneous and heterogeneous chemical reactions. During these processes, formation of nanoparticles follows as a result of nucleus formation from supersaturated inorganic vapors and further growth of nanoparticles via collisions and chemical reactions on the surface.

Evaporation of raw particles is the limiting stage in nanoparticle production rate. To avoid product contamination, all the raw material has to be evaporated.

The conditions in reaction zone for each type of plasma source are determined by temperature and velocity distributions in plasma jet at the reactor's entrance and raw material injection conditions (position relative to plasma jet inlet, injection angle, and injection velocity).

Evaporation rate is affected by temperature difference between plasma flow and raw particle, relative particle velocity, and particle size. High level of turbulent pulsations in hot gas stream also has positive influence on the evaporation rate.

Due to increase of heat and mass transfer rates in the jet collision zone, multijet reactors with self-impinged jets were successfully used for process intensification in various chemical processes. de Gelicourt et al. [30] have used impinging jet reactor for precipitation of nanoparticles in liquid streams.

Plasma reactors with three plasma jets' impingement in the mixing chamber were used for solid materials processing [31] and for synthesis of chromium carbides and nitrides [32].

The main objective of this work is therefore to appraise the ability of titanium carbonitride synthesis in plasma reactor with multijet configuration.

This article is structured as follows: in the next section, the description of the experimental setup and experimental conditions is given. Methods of chemical, phase, and morphologic analyses are listed in the following section.

Further results of experiments including influence of process operational parameters ($C : TiO_2$ ratio) on chemical composition, phase composition particles size, and morphology are described.

In the next section the simulated flow structure, particle trajectories, and thermal histories in the reactor are reported and discussed. Conclusions are summarized in the final section.

This paper reports on the peculiarities of titanium carbonitride nanopowder synthesis in a multijet plasmachemical reactor operating with nitrogen as plasma forming gas and using titanium dioxide as titanium-bearing raw material and natural gas (propane-butane mixture) as source of carbon. Technical quality nitrogen (98% purity) was used. Systematic

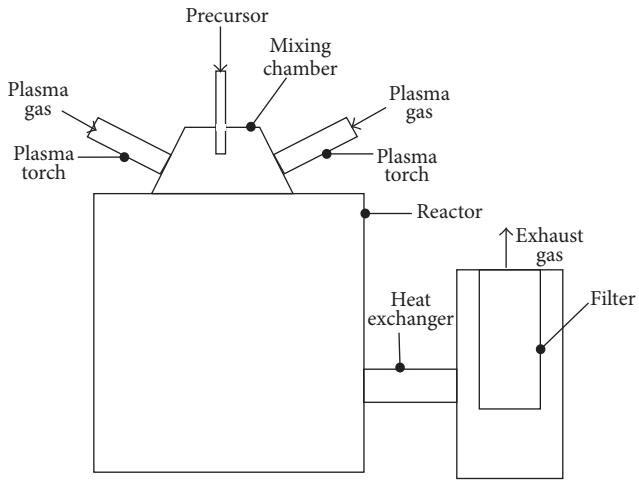

Figure 1: Multijet plasma reactor.

investigation into the effects of the process parameters on the formation of Ti(C, N) was carried out.

2. Materials and Methods

2.1. Experimental Setup. A schematic diagram of experimental setup for the production of titanium carbonitride nanoparticles is shown in Figure 1. The system consists of the three DC plasma torches EDP-104A [33], mixing chamber, reactor, heat exchanger, and particle collection filter. Nitrogen was used as plasma forming gas.

Feed powder (precursor) was technical grade titania (particle size less 20 microns, purity 99%). Precursor particles were fed into the mixing chamber by two-phase jet (mixture of nitrogen and propane-butane). Once particles are injected into the zone of three plasma jets' collision, the particles underwent intensive heating and eventually they were evaporated due to the high enthalpy of the thermal plasma and heterogeneous chemical reactions on the surface of the particles. Concurrently with evaporation vapors of the injected titania and products of chemical reaction were transported by the plasma flow from mixing chamber into the reactor volume. Due to rapid temperature decrease in the stream, formed by plasma jets collision, the vapors became supersaturated leading to onset of nucleation. The formed nucleus served as centers of the subsequent condensation. The nanopowder formed fluffy deposition layers on the walls of the mixing chamber, reactor, and heat exchanger. The nanoproducts were collected from the water-cooled walls of the reactor and from the filter.

Chemical and phase composition of titania conversion products are dependent on synthesis conditions in the mixing chamber and reactor, such as components concentrations, temperature, and velocity spatial distributions.

For the given type of mixing chamber the synthesis conditions depend on raw material concentrations at the precursor injection port, temperature and velocity spatial distributions in plasma jets, and plasma jet injection angle.

Table 1: Experimental conditions.

Parameter	Value
Plasma jet mean mass temperature, K	5700–5800
Angle between plasma jet axis and reactor's axis, degrees	60
Plasma jet dynamic pressure P_{plasma}, Pa	46320–47000
Two-phase jet dynamic pressure, $P_{\text{two-phase}}$, Pa	463–7520
Dynamic pressures ratio $\Psi = P_{\text{two-phase}}/P_{\text{plasma}}$	0.01–0.16
Propane-butane mixture flow rate, m^3/h	0.26–0.46
$C : TiO_2$ ratio, mole/mole	2.0–4.8
Nitrogen carrier gas flow rate, m^3/h	0.8
Titanium dioxide flow rate, kg/h	1.2–4.0

To control the synthesis conditions, the following parameters were varied:

(a) Mole ratio $C : TiO_2$ in the two-phase jet (propane-butane mixture and titania particles).

(b) Parameter Ψ (see (2) below) representing ratio of dynamic pressures between two-phase jet and plasma jet.

The calculations of mean mass velocities U and dynamic pressures of plasma jet and two-phase jet P_{jet} were done according to the following equations:

$$U = \frac{\sum_i V_i}{A},$$
$$P_{\text{jet}} = U\frac{\sum_i G_i}{A}. \quad (1)$$

The dynamic pressures ratio Ψ was calculated according to the following equation:

$$\Psi = \frac{P_{\text{two-phase jet}}}{P_{\text{plasma jet}}}, \quad (2)$$

where V_i is volumetric flow rates of each jet, G_i is mass flow rate of a gas component (nitrogen, propane-butane mixture), and A is the area of the plasma jet or injection port.

The experimental conditions are given in Table 1.

The synthesized nanopowder was characterized by chemical analysis (mass content of Ti, O, N, and C). Phase composition was investigated by X-ray diffractometry data (XRD) analysis. Oxygen, nitrogen, and total carbon content were measured by LECO analyzers (LECO Corporation, St. Joseph, MI, USA). The free carbon in product was extracted by wet chemical method and its contents in the solution were measured using element analyzer (AN-7529). The fixed carbon content was measured by the difference in the contents of the total and free carbon [34].

The morphology of the particles was observed with the help of transmission electron microscopy (TEM) using

Table 2: Phase composition of nanoproducts.

Mole ratio C : TiO_2	Lattice parameter $TiC_xN_yO_z$, nm	Composition of each phase	Phase mass ratio	Titania content, mass%
2.0	0.4261/0.4243	$TiC_{0.25}(N,O)_{0.75}$ $TiC_{0.05}(N,O)_{0.95}$	0.80/0.20	—
4.5	0.4307/0.4257	$TiC_{0.76}(N,O)_{0.24}$ $TiC_{0.20}(N,O)_{0.80}$	0.83/0.17	0.2

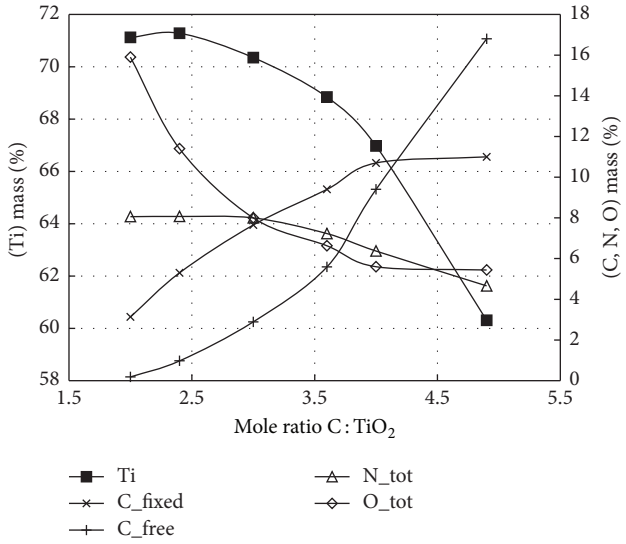

Figure 2: Chemical composition of nanoproducts versus mole ratio C : TiO_2 (dynamic pressure ratio $\Psi = 2.5$).

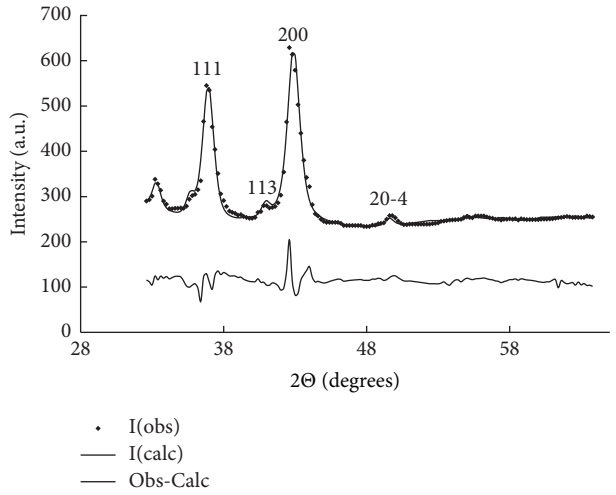

Figure 3: XRD plot of nanopowder refined by Rietveld method. I(obs) represents the experimentally observed points, passing through the points; black line I(calc) represents observed X-ray diffraction pattern fitted by an exponential pseudo-Voigt convolution; black thin line (Obs-Calc) below the observed points represents difference plot.

microscope JEM-100X, JEOL Ltd. Quantitative phase analysis by XRD was carried out with the help of DRON-3 diffractometer (Cu-Kα).

The results of experiments are given in Figure 2 and Table 2.

2.2. Chemical Composition. The increase of the propane-butane mixture volumetric flow rate from 0.26 to 0.46 m^3/h (mole ratio C : TiO_2 = 2.0–4.8 mol/mol) leads to increase of the total carbon and fixed nitrogen content in the synthesized nanopowder and at the same time leads to the decrease of the oxygen content and titanium content. Chemically bonded carbon (C_{fixed}) content depends upon mole ratio C : TiO_2 and is increased with the growth of the later. The concentration of the free carbon reaches 16 mass% at the ratio C : TiO_2 = 4.8 mol/mol.

2.3. Phase Composition. Both titanium nitride and titanium carbide have crystal structure with NaCl type lattice. They can form an infinite series of solid solutions where atoms of nonmetals substitute each other. Phase diagrams of the TiC-TiN system show wide region of solubility of TiC in TiN, indicating possibility of solid solution formation.

The XRD results are given in Table 2, demonstrating formation of titanium oxycarbonitride with crystal lattice parameter varying in the range 0.4243–0.4307 nm.

The nanopowder consists of two phases: one phase with higher carbon index x and another phase with lower carbon index x. Mass fraction of the phase with higher carbon index x is about 4–4.7 times higher than mass fraction of another phase (see Table 2), which indicates existence of two zones in reactor with different reaction conditions (temperature distribution, residence time, etc.). Fixed carbon content increased with increase of mole ratio C : TiO_2. At the same values of the molar ratio C : TiO_2 higher amounts of carbon are chemically bonded in the titanium oxycarbonitride nanopowder.

GSAS package of programs [35] was used for Rietveld refinement of the recorded X-ray data profile. The reflection profiles were fitted by an exponential pseudo-Voigt convolution as implemented in the free software GSAS.

Typical XRD pattern of synthesized powder is shown in Figure 3. I(obs) points and I(calc) black line represent observed X-ray diffraction pattern fitted by an exponential pseudo-Voigt convolution. Profile fitting is a technique used to extract precise information about the position, intensity, width, and shape of each individual peak in a diffraction pattern. The peak information can be used in several calculations to quantify sample parameters such as unit cell lattice parameters, crystallite size and microstrain, and relative weight fractions. Black thin line (Obs-Calc) represents difference plot. The difference plot shows where the greatest differences between the experimental plot and calculated pseudo-Voigt plot are.

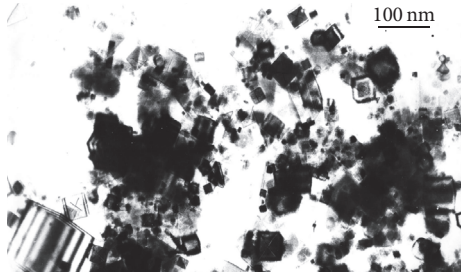

Figure 4: Morphology of TiC(N,O) nanoparticles. Nanoparticles have cubic shape.

XRD results in Figure 3 show presence of the compounds with variable chemical composition, such as titanium oxycarbonitride ($2\Theta = 36.5$, 42.5 degrees, peaks 111, 200) and traces of titanium oxide Ti_2O_3 ($2\Theta = 39.6$, 49.5 degrees, peaks 113, 20-4). Titanium oxycarbonitride lattice parameter varied in the range 0.4243–0.4307 nm.

The data in Table 2 suggests that the increase of the propane-butane mixture flow rate creates necessary conditions for formation of the two different titanium oxycarbonitride compositions. As results of previous thermodynamic calculations indicate, formation of $TiC_x(N,O)_y$ phases with high carbon index x ($x > 0.8$) occurs in the high-temperature zone and higher $C : TiO_2$ molar ratio, while lower temperatures and lower $C : TiO_2$ molar ratio favor formation of phases with low carbon index. The chemical analysis of the fixed carbon also indicates the existence of titanium oxycarbonitride.

CFD calculations demonstrate existence of higher temperatures near the reactor axis and lower temperatures near the water-cooled walls. Due to temperature gradients it is possible that raw material particles travelling in the higher temperature zone take part in the formation of phases with high carbon index, while particles moving in near-wall region participate in formation of phases with low carbon index.

2.4. Nanopowder Morphology and Particle Size. The synthesized nanoparticles (less than 100 nm) have cubical shape and they are covered by a layer of amorphous carbon (see Figure 4).

Specific surface area (SSA) of nanoproducts was measured by BET method. SSA varied in the range 29–61 m^2/g.

Typical BET line graph for titanium carbonitride nanopowder using nitrogen as adsorbed gas was prepared with TriStar 3000 instrument (Micrometrics Instrument Corporation) and is shown in Figure 5. Standard method to calculate the specific surface area from measured BET line as supplied in the instrument manual was used.

2.5. Theoretical: Flow and Temperature Fields in Multijet Reactor via Computational Fluid Dynamics (CFD). CFD simulations served as a tool to achieve some understanding of flow structure and particle trajectories and thermal histories in the reactor. Also it was possible to gain better insight into operation conditions, when dynamic pressures ratio between two-phase jet and plasma jets allowed solid precursor particles to penetrate into and pass through the plasma jets collision zone

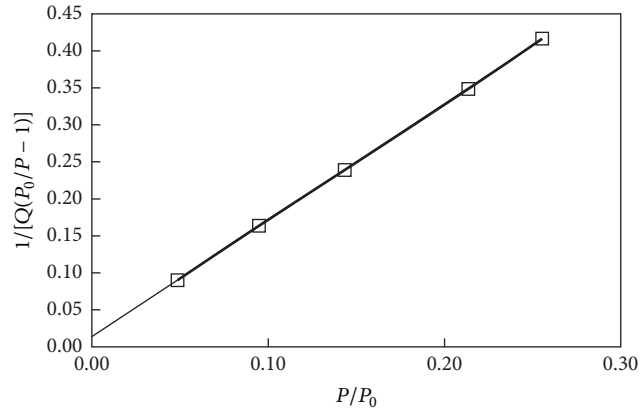

Figure 5: BET line for Ti(C,N,O) nanopowder with specific surface area 61 m^2/g.

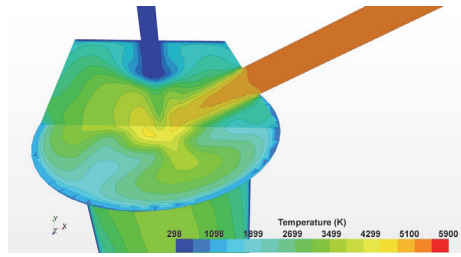

Figure 6: Temperature distributions in mixing chamber and in the reactor volume.

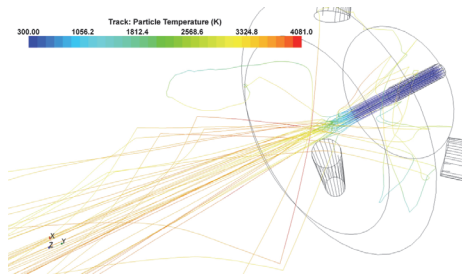

Figure 7: Titanium dioxide particles tracks and temperature histories in the reactor volume.

and move further in the downstream flow (see Figures 6 and 7). CFD simulations of titanium dioxide particles movement in pure nitrogen were carried out using commercial code STAR-CCM+ ver.8. Full Reynolds stress model for turbulence simulation and Lagrange particle tracking method with two-way momentum and heat transfer coupling were used.

Giving complexity of the real process, the results of CFD simulation should be considered as qualitative, but indicating process trends.

The layout of the simulated setup is given in Figure 1, and reactor and mixing chamber dimensions are given in Table 3.

The proper selection of raw material injection velocity is highly important for the steady operation of the reactor.

To evaluate the required injection velocity, some calculations of flow pattern in the mixing chamber were carried out.

Table 3: Design parameters of the mixing chamber and reactor.

Design parameter	Value
Conical mixing chamber upper/lower inner diameter, m	0.05/0.127
Conical mixing chamber length, m	0.190
Reactor inner diameter, m	0.4
Reactor length, m	0.5
Angle between plasma jet axis and reactor axis, degrees	60
Precursor injection port diameter, m	0.004
Plasma torch outlet electrode diameter, m	0.018

The calculations revealed that high pressure core is formed as a result of plasma jets collision. After plasma jets self-impingement, two main flow directions are observed, namely, axial upstream and axial downstream flows. The formation of the upstream flow, which is directed oppositely to the particle injection velocity vector, could prevent raw material particles penetration into the high pressure core and further movement along the axis of reactor. The velocity in the downstream flow determines the residence time of raw titanium dioxide particles in the high-temperature zone, where evaporation takes place. Temperatures in the central region of reactor and mixing chamber exceed $T = 2900$ K which is phase transition temperature of titanium dioxide in inert media (Figure 6).

The amount of titania particles colliding with the mixing chamber wall above plasma jet collision zone is significantly lower than amount of particles moving downstream through the plasma jet collision zone. At injection velocity 30 m/s ($C : TiO_2 = 3$) particle trajectories cross the plasma jets collision zone and particles move further in the axial direction. No particles impingement on mixing chamber walls is observed. Particles are heated by plasma jets up to 3400 K (see Figure 7).

High gas turbulent kinetic energy in the plasma jet mixing zone allows fast heating of solid precursor particles ensuring conversion of the titanium dioxide particles into titanium carbonitride nanopowder. Particle temperature rises up to 3000–3400 K, which is sufficient for titania evaporation in chemically active media as shown by previous thermodynamical calculations.

When raw solid particles are injected in the mixing chamber at sufficient injection velocity, they can penetrate into the plasma jets collision zone and move further along with downstream flow. The actual particles trajectories will be determined by the ratio of the upstream flow dynamic pressure and dynamic pressure of the two-phase jet with raw material. The particles residence time in the zone confined by isotherm 2300 K (titania phase transition temperature in chemically active media) varies in the range 12–25 msec, and residence time in the zone confined by isotherm 2900 K (titania phase transition temperature in inert media) varies in the range 5–12 msec.

3. Results and Discussion

Experimental work demonstrated that in the three-jet chemical reactor with self-impingement plasma jets it was possible to synthesize titanium carbonitride consisting of two phases at high production rates up to 4 kg/h using nitrogen plasma, propane-butane mixture, and titania as raw materials. XRD analysis revealed that titanium carbide composition prevailed in one phase, and titanium nitride composition was dominating in another phase.

Phase composition varied in the range $TiC_{0.76}(N,O)_{0.24}$–$TiC_{0.25}(N,O)_{0.75}$. Molar ratio $C : TiO_2$ was found to be the main process parameter, which influences the chemical and phase composition. The existence of two phases in the product could be explained by different trajectories of evaporating precursor particles and hence different temperatures and chemical species concentration in the reactor, as indicated by CFD calculations.

The experimental results have shown that at the precursor feed rate 2 kg/h the titanium carbonitride production rate achieved 1.4 kg/h. The increase of the titanium dioxide feed rate above 3 kg/h when the input electrical power was equal to 60 kW reduced the nanopowder yield and unreacted precursor appeared in the product. When content of free carbon C_{free} increases from 0.4 to 18%, the specific area of the nanoproducts increased from 29 to 50 m^2/g. No sintering of the nanoparticles deposited on the settling chamber walls was observed. The thickness of the deposition layer varied in the range 4–8 mm. No difference in chemical composition between filter products and settling chamber products was observed. The increase of reactor diameter after the zone of plasma jet collision (sudden channel expansion) allowed preventing skull formation on the water-cooled walls and performing synthesis in a steady mode, while providing fixed carbon content of the nanoproducts in the range 6–11 mass%.

The following operational and design parameters do influence the phase and chemical composition of the synthesized product:

(1) Molar ratio $C : TiO_2$: When the ratio $C : TiO_2$ is higher than 4, it facilitates formation of TiC_x rich phase in the nanoproducts (carbon index x increases up to 0.76), but free carbon content also increases.

(2) The ratio of hydrodynamics pressures of the two-phase jet with feed material and plasma jet Ψ determines penetration of raw titania particles through the plasma jet collision zone and the following particles thermal and spatial history in the reactor. The increase of Ψ in the range 0.01–0.2 reduces probability of skull formation on the mixing chamber walls above plasma jet collision zone.

(3) At the input electrical power level 60 kW and plasma jet intersection angle 60° the conversion of TiO_2 into Ti(C,N,O) is close to 100% at the precursor feed rates in the range 1.4–2 kg/h.

(4) The chemical composition of the synthesized nanoproducts varies amongst $TiC_{0.76}(N,O)_{0.24}$–$TiC_{0.25}(N,O)_{0.75}$. Most of the synthesized nanoparticles have size in the range 10–80 nm, and free carbon content varies in the range 0.1–19 mass%. The synthesized nanoparticles have prevailing cubic shape.

(5) CFD simulations revealed particle trajectories and confirmed that at plasma jet collision angle 60° and reactor with diameter much larger than mixing chamber diameter (sudden flow expansion), almost all the raw titania particles penetrate plasma jet collision zone and the number of particles collisions with the chamber and reactor walls is small. Such reactor-mixing chamber configuration allows avoiding skull formation on the walls and achieves steady operation.

Competing Interests

The authors declare that there is no conflict of interests regarding the publication of this paper.

Acknowledgments

The authors would like to thank Professor M. Lototskyy (University of Western Cape) for the help with XRD processing and interpretations.

References

[1] H. Pastor, "Titanium-carbonitride-based hard alloys for cutting tools," *Materials Science and Engineering*, vol. 105-106, no. 2, pp. 401–409, 1988.

[2] P. Ettmayer, H. Kolaska, W. Lengauer, and K. Dreyer, "Ti(C,N) cermets—metallurgy and properties," *International Journal of Refractory Metals and Hard Materials*, vol. 13, no. 6, pp. 343–351, 1995.

[3] K. Wang, H. Jiang, Q. Wang, B. Ye, and W. Ding, "Nanoparticle-induced nucleation of eutectic silicon in hypoeutectic Al-Si alloy," *Materials Characterization*, vol. 117, pp. 41–46, 2016.

[4] A. M. Orishich, A. G. Malikov, and A. N. Cherepanov, "Effect of nanopowder modifiers on properties of metal laser-welded joints," *Physics Procedia*, vol. 56, pp. 507–514, 2014.

[5] V. T. Kalinin, V. E. Khrychikov, and V. A. Krivosheev, "Theory and practice of cast-iron inoculation by ultra—and nanodispersed materials," *Metallurgical and Mining Industry*, vol. 2, no. 5, pp. 341–347, 2010 (Russian).

[6] G. G. Krushenko and M. N. Filkov, "Modification of aluminium alloys by nanopowders," *Nanotechnics*, vol. 4, no. 12, pp. 58–64, 2007 (Russian).

[7] G. G. Krushenko and M. N. Filkov, "Application of titanium nitride nanopowder to obtain complex-loaded cast details of aluminium-silicon alloys with required mechanical properties," *Nanotechnics*, vol. 3, no. 15, pp. 77–79, 2004 (Russian).

[8] V. P. Saburov, E. N. Eremin, A. N. Cherepanov et al., *Modifying Steels and Alloys by Dispersed Inoculators*, Omsk State Technical University, Omsk, Russia, 2002.

[9] G. Krushenko and M. Filkov, "Avoiding crust on the steel and casted iron ingots by applying parting compounds with refractory nanoparticles," *Industrial Ecology (Ekologia promyshlennogo proizvodstva, in Russian)*, vol. 4, pp. 43–46, 2010.

[10] *Plasmachemical Synthesis of Ultrafine Powders and Applications for Metals and Alloys Inoculation*, Nauka, Novosibirsk, Russia, 1995.

[11] M. Rieth, *Nano-Engineering in Science and Technology: An Introduction to the World of Nano-Design*, Series on the Foundations of Natural Science and Technology, World Scientific, Singapore, 2003.

[12] G. G. Krushenko and M. N. Filkov, "Modifying rods with increased content of nanopowders," *Manufacturing Engineering (Technologiya Mashinostroeniya)*, no. 5, pp. 5–9, 2011 (Russian).

[13] N. V. Alekseev, I. L. Balikhin, E. N. Kurkin, A. V. Samokhin, E. V. Troitskaya, and V. N. Troitskij, "Synthesis of titanium nitride and carbonitride ultra-fine powders from titanium hydride in nitrogen arc discharge plasma jet," *Fizika i Khimiya Obrabotki Materialov*, no. 1, pp. 31–39, 1995.

[14] N. V. Alekseev, A. V. Samokhin, and Y. V. Tsvetkov, "Synthesis of titanium carbonitride nanopowder," *High Energy Chemistry*, vol. 33, no. 3, pp. 194–197, 1999.

[15] A. V. Samokhin, V. A. Sinaiskii, N. V. Alekseev, E. V. Troitskaya, and Y. V. Tsvetkov, "Production of titanium nitride nanopowder from titanium hydride based on synthesis in thermal plasma," *Inorganic Materials: Applied Research*, vol. 5, no. 3, pp. 224–229, 2014.

[16] J. Slifirski and F. Teyssandier, "Titanium carbide and titanium carbonitride obtained by chemical vapor deposition from orgranometallic precursor in the range 450–800°C," *Journal De Physique*, vol. 3, no. 3, pp. 367–374, 1993.

[17] X. L. Chen, Y. B. Li, Y. W. Li et al., "Carbothermic reduction synthesis of Ti(C, N) powder in the presence of molten salt," *Ceramics International*, vol. 34, no. 5, pp. 1253–1259, 2008.

[18] D. Xiang, Y. Liu, Z. Zhao, H. Cao, S. Gao, and M. Tu, "Reaction sequences and influence factors during preparation of Ti(C,N) powders," *Journal of Alloys and Compounds*, vol. 429, no. 1-2, pp. 264–269, 2007.

[19] J. Xiang, Z. Xie, Y. Huang, and H. Xiao, "Synthesis of Ti(C,N) ultrafine powders by carbothermal reduction of TiO_2 derived from sol-gel process," *Journal of the European Ceramic Society*, vol. 20, no. 7, pp. 933–938, 2000.

[20] F.-S. Yin, L. Zhou, Z.-F. Xu, B. Xue, and X.-B. Jiang, "Synthesis of nanocrystalline titanium carbonitride during milling of titanium and carbon in nitrogen atmosphere," *Journal of Alloys and Compounds*, vol. 470, no. 1-2, pp. 369–374, 2009.

[21] A. V. Samokhin, N. V. Alekseev, and Y. V. Tsvetkov, "Plasma-assisted processes for manufacturing nanosized powder materials," *High Energy Chemistry*, vol. 40, no. 2, pp. 93–97, 2006.

[22] A. V. Bolotov, V. N. Musolin, A. V. Kolesnikov et al., "Multi-jet plasmachemical reactor: the possibility to control the chemical and phase compositiion of titanium carbonitride," in *Proceedings of the 6th International Symposium on Plasma Chemistry (ISPC '83)*, pp. 237–340, Montreal, Canada, July 1983.

[23] J. Grabis and I. Zalite, "Preparation of Ti(N, C) based nanosized powders and their densification," *Materials Science (Medžiagotyra)*, vol. 11, no. 4, pp. 372–375, 2005.

[24] I. Zalite, J. Grabis, E. Palcevskis et al., "Plasma processed nanosized-powders of refractory compounds for obtaining fine-grained advanced ceramics," *IOP Conference Series: Materials Science and Engineering*, vol. 18, no. 6, 2011.

[25] I. Zalite and J. Krastins, "Preparation and properties of nanodisperse transition metals carbonitrides," in *Proceedings of the 15th International Plansee Seminar*, pp. 340–351, Reutte, Austria, 2001.

[26] A. N. Ermakov, *Phase formation in the system nanosized TiCN-TiNi [Ph.D. thesis]*, Ural Institute of Solid State Chemistry, Yekaterinburg, Russia, 2004.

[27] M. Leparoux, Y. Leconte, A. Wirth, and T. Buehler, "In situ treatment of thermal RF plasma processed nanopowders to control their agglomeration and dispersability," *Plasma Chemistry and Plasma Processing*, vol. 30, no. 6, pp. 779–793, 2010.

[28] M. Leparoux, Y. Kihn, S. Paris, and C. Schreuders, "Microstructure analysis of RF plasma synthesized TiCN nanopowders," *International Journal of Refractory Metals and Hard Materials*, vol. 26, no. 4, pp. 277–285, 2008.

[29] J. S. McFeaters, R. L. Stephens, P. Schwerdtfeger, and M. Liddell, "Numerical modeling of titanium carbide synthesis in thermal plasma reactors," *Plasma Chemistry and Plasma Processing*, vol. 14, no. 3, pp. 333–360, 1994.

[30] Y. S. de Gelicourt, D. L. Marchisio, A. A. Barresi et al., "CFD modeling of precipitation of nanoparticles in confined impinging jet reactors," in *Proceedings of the Computational Fluid Dynamics in Chemical Reaction Engineering Conference*, Barga, Italy, 2005.

[31] I. I. Krasovskaya and M. A. Brich, "Numerical modeling of the thermal and gasdynamic structure of plasma flows in reactors with three-jet mixing chambers," *Journal of Engineering Physics and Thermophysics*, vol. 74, no. 5, pp. 108–114, 2001.

[32] L. S. Shiryaeva, I. V. Nozdrin, and G. V. Galevsky, "Peculiarities of production of chromium carbonitride nanopowder and its physical-chemical certification," in *Proceedings of the 6th International Scientific Practical Conference on Innovative Technologies and Economics in Engineering*, vol. 91, no. 1, May 2015.

[33] *Thermal Plasma Torches and Technologies (in two volumes)*, Cambridge International Science, London, UK, 2000.

[34] D. W. Lee, S. Alexandrovskii, and B. K. Kim, "Mg-thermal reduction of $TiCl_4$+C_xCl_4 solution for producing ultrafine titanium carbide," *Materials Chemistry and Physics*, vol. 88, no. 1, pp. 23–26, 2004.

[35] A. C. Larson and R. B. Von Dreele, "General Structure Analysis System (GSAS)," Report LAUR 86-748 LAUR 86-748, Alamos National Laboratory, Los Alamos, NM, USA, 2004.